18F-Fluoroestradiol PET Imaging in a Phase II Trial of Vorinostat to Restore Endocrine Sensitivity in ER+/HER2− Metastatic Breast Cancer

Lanell M. Peterson[1], Brenda F. Kurland[2], Fengting Yan[1], Alena Novakova- Jiresova[3], Vijayakrishna K. Gadi[1,4], Jennifer M. Specht[1], Julie R. Gralow[1], Erin K. Schubert[5], Jeanne M. Link[6], Kenneth A. Krohn[6], Janet F. Eary[7], David A. Mankoff[5], and Hannah M. Linden[1]

[1]Division of Medical Oncology, University of Washington/Seattle Cancer Care Alliance, Seattle, Washington; [2]Department of Biostatistics, University of Pittsburgh, Pittsburgh, Pennsylvania; [3]Department of Oncology, First Faculty of Medicine, Charles University and Thomayer Hospital, Prague, Czech Republic; [4]Clinical Research and Public Health Sciences Division, Fred Hutchinson Cancer Research Center, Seattle, Washington; [5]Department of Radiology, University of Pennsylvania, Philadelphia, Pennsylvania; [6]Department of Diagnostic Radiology, Oregon Health and Science University, Portland, Oregon; and [7]Cancer Imaging Program, National Cancer Institute, Bethesda, Maryland

Histone deacetylase inhibitors (HDACIs) may overcome endocrine resistance in estrogen receptor–positive (ER+) metastatic breast cancer. We tested whether 18F-fluoroestradiol PET imaging would elucidate the pharmacodynamics of combination HDACIs and endocrine therapy. **Methods:** Patients with ER+/human epidermal growth factor receptor 2 (HER2)–negative metastatic breast cancer with prior clinical benefit from endocrine therapy but later progression on aromatase inhibitor (AI) therapy were given vorinostat (400 mg daily) sequentially or simultaneously with AI. 18F-fluoroestradiol PET and 18F-FDG PET scans were performed at baseline, week 2, and week 8. **Results:** Eight patients were treated sequentially, and then 15 simultaneously. Eight patients had stable disease at week 8, and 6 of these 8 patients had more than 6 mo of stable disease. Higher baseline 18F-fluoroestradiol uptake was associated with longer progression-free survival. 18F-fluoroestradiol uptake did not systematically increase with vorinostat exposure, indicating no change in regional ER estradiol binding, and 18F-FDG uptake did not show a significant decrease, as would have been expected with tumor regression. **Conclusion:** Simultaneous HDACIs and AI dosing in patients with cancer resistant to AI alone showed clinical benefit (6 or more months without progression) in 4 of 10 evaluable patients. Higher 18F-fluoroestradiol PET uptake identified patients likely to benefit from combination therapy, but vorinostat did not change ER expression at the level of detection of 18F-fluoroestradiol PET.

Key Words: FES; vorinostat; ER+ breast cancer; metastatic breast cancer; estrogen receptors

Nearly two thirds of invasive breast carcinomas express the estrogen receptor (ER) (1). Endocrine therapy is the mainstay of treatment for these tumors, because of a favorable toxicity profile and efficacy. For postmenopausal women with advanced or metastatic hormone receptor–positive disease, whose disease is considered treatable but not curable, the initial standard-of-care treatment is aromatase inhibitors (AIs) with or without cyclin-dependent kinase 4/6 inhibition (2). On progression, salvage endocrine therapy with molecularly targeted agents or chemotherapy is indicated (3). Recent phase III trials combining later-line endocrine therapy with a targeted agent, such as palbociclib, alpelisib, or everolimus, have demonstrated considerable improvement in outcome (4–6) over endocrine therapy alone.

Epigenetic modulation by histone deacetylase inhibitors (HDACIs) has been proposed as a mechanism to reverse endocrine resistance (7). The transcription of ERs is regulated by epigenetic modifications, including histone deacetylases, and HDACIs reverse resistance to antiestrogen therapies in vitro (8–12). HDACI activity has been shown to increase breast cancer drug sensitivity in vitro (13,14), and cell lines engineered for endocrine resistance demonstrated restored endocrine sensitivity after treatment with an HDACI (7,15).

Clinical studies have shown promising results when combining endocrine therapy with HDACIs, including exemestane with entinostat (16), tamoxifen with vorinostat (17), and a randomized phase III study (NCI-E2112; trial NCT02115282 at Clinical-Trials.gov) of endocrine therapy plus entinostat or placebo in patients with hormone receptor–positive advanced breast cancer (18).

18F-fluoroestradiol PET measures ER status (19,20), and 18F-fluoroestradiol uptake predicts response to endocrine therapy (21–24). 18F-FDG PET measures tumor glycolytic activity; a decrease in 18F-FDG PET has been shown to be a robust measure of early response of breast cancer to endocrine therapy and chemotherapy (25,26) and is prognostic in metastatic breast cancer (27–29). We hypothesized that serial 18F-fluoroestradiol and 18F-FDG PET imaging could assess restored endocrine sensitivity in patients with ER+ tumors with prior clinical benefit from
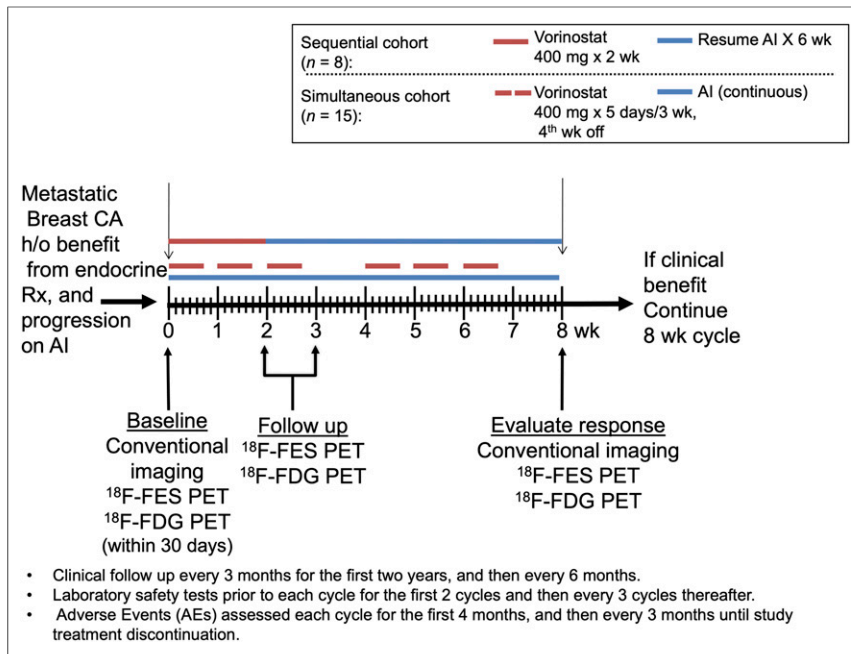
FIGURE 1. Study schema. CA = cancer; h/o = history of; Rx = therapy.

endocrine therapy but later progression on an AI and could be used to predict treatment response.

Vorinostat is a potent HDACI targeting class 1 and 2 histone deacetylases, with antitumor activity seen in phase I trials (30). However, a phase II trial to determine the response rate of single-agent vorinostat (200 mg orally twice daily, administered for the first 14 d of each 21-d cycle) in 14 patients with stage IV metastatic breast cancer failed to reach its primary endpoint (31), suggesting that ER targeting in addition to HDACIs may be essential. Vorinostat combined with endocrine therapy has shown promise (16,17), suggesting that HDACIs might be combined with AIs to effectively target ER+ tumors and potentially overcome resistance in patients whose tumors may have endocrine sensitivity. The combination of HDACIs in synergy with AI may result in resensitization to endocrine therapy.

We used correlative molecular imaging (^{18}F-fluoroestradiol PET and FDG PET) in our study of combined vorinostat and AI therapy, to examine the impact of HDACIs on tumor ER expression and metabolism.

MATERIALS AND METHODS

Patients

Eligible patients had metastatic breast cancer and were required to have had documentation of prior clinical benefit from endocrine therapy and subsequent progression while on an AI. Prior chemotherapy was allowed. Patients agreed to a study of AI therapy with vorinostat, imaging with ^{18}F-fluoroestradiol PET and ^{18}F-FDG PET, and clinical follow-up of up to 5 y. The institutional review board approved this study, and all subjects gave written informed consent. Additional eligibility criteria are shown in Supplemental Table 1 (supplemental materials are available at http://jnm.snmjournals.org).

Study Design and Treatment Plan

An open-label phase II clinical trial was conducted on 2 cohorts. Initially, patients were given vorinostat, 400 mg orally daily for 2 wk, followed by an AI daily for 6 wk. As emerging data demonstrated the

safety of concurrent vorinostat with endocrine therapy (17), the study protocol was modified to simultaneous administration: 400 mg of vorinostat daily for 5 consecutive days in 3 wk, with fourth week off, in two 28-d cycles and given concomitantly with the daily AI, as illustrated in Figure 1.

Paired ^{18}F-fluoroestradiol PET and ^{18}F-FDG PET were performed at baseline, 2 wk, and 8 wk of treatment as shown in Figure 1. Conventional imaging (CT, bone scanning) was performed at baseline and at week 8, and tumor response was assessed by RECIST in patients with measurable disease or clinical signs of progression (32). Patients were also followed for progression-free survival (PFS). Patients with response or stable disease were offered continuation of study treatment on the same schedule until disease progression, unacceptable toxicity, or study withdrawal.

[18]F-fluoroestradiol was synthesized at the University of Washington according to the requirements for investigational new drug 101203, as previously described (32). ^{18}F-FDG was purchased commercially from Cardinal Health. All doses underwent quality control testing before injection.

[18]F-fluoroestradiol PET imaging was performed as previously described (32). ^{18}F-FDG PET imaging was performed according to the clinical protocol. All imaging was done on a whole-body PET scanner (Advance; GE Healthcare) or PET/CT scanner (Discovery STE; GE Healthcare). Torso surveys covering 5 adjacent 15-cm axial fields of view beginning approximately 60 min after isotope injection were used for analysis.

Image Analysis

[18]F-fluoroestradiol PET scans were qualitatively and quantitatively analyzed. For each site of active disease, 2 trained observers masked to the clinical data but with access to ^{18}F-FDG PET and other correlative imaging studies qualitatively determined if ^{18}F-fluoroestradiol uptake above background levels was present at known sites of disease. Any differences between observers were resolved by consensus, with only 1 value recorded. Analysis of ^{18}F-fluoroestradiol and ^{18}F-FDG PET images was based on prior experience using combined imaging to predict endocrine responsiveness (23). Uptake was quantified using lean body mass–adjusted (33) SUV_{mean} (SUL_{mean}) for ^{18}F-fluoroestradiol and SUV_{max} for ^{18}F-FDG. Regions of interest were generated around the SUV_{max} for ^{18}F-FDG studies. Regions of interest of approximately 1.5-cm diameter were drawn on 3 adjacent planes using PMOD software on the ^{18}F-fluoroestradiol images over the same lesions as in the ^{18}F-FDG images. Up to 10 lesion sites on the static torso survey were quantified. Predefined patient-level summaries were selected on the basis of the results of a prior study in which a patient-level ^{18}F-fluoroestradiol uptake summary (SUL_{mean}) of less than 0.85 predicted inferior PFS on endocrine monotherapy for patients with an ^{18}F-FDG SUV_{max} of 2.2 or greater (23). These patient-level summaries were the geometric mean for up to 3 lesions with the highest ^{18}F-FDG SUV_{max}:

Patient-level ^{18}F-fluoroestradiol uptake summary =

$$\text{antilog}\left[\left(\sum_{1}^{n_i}\log(^{18}\text{F} - \text{FES } SUL_{mean})/n_i\right)\right] \text{ Eq. 1}$$

TABLE 1
Patient Characteristics at Enrollment

Characteristic	Data
Sequential cohort ($n = 8$)	
Age (y)	55 (44–74)
Duration of metastatic disease (y)	5 (2–12)
Prior chemotherapy regimens (neoadjuvant, adjuvant, metastatic)	3.5 (1–9)
Prior endocrine regimens	4.5 (2–6)
Number of lesions	5 (2–9)
Sites of disease	
Soft tissue or bone	6 (75%)
Includes visceral disease (lung or liver lesions)	2 (25%)
Average ^{18}F-FDG SUV$_{max}$*	4.7 (3.6–9.9)
Average ^{18}F-fluoroestradiol SULmean*	1.3 (0.6–4.0)
Average ^{18}F-fluoroestradiol SUV$_{max}$	3.3 (1.9–7.6)
Simultaneous cohort ($n = 15$)	
Age (y)	65 (32–76)
Duration of metastatic disease (y)	4 (0.5–10)
Prior chemotherapy regimens (neoadjuvant, adjuvant, metastatic)	4 (2–10)
Prior endocrine regimens	3 (2–5)
Number of lesions	7 (1–10)
Sites of disease	
Soft tissue only	2 (13%)
Soft tissue or bone	6 (40%)
Includes visceral disease (lung or liver lesions)	7 (47%)
Average ^{18}F-FDG SUV$_{max}$*	5.2 (2.7–12.8)
Average ^{18}F-fluoroestradiol SULmean*	1.2 (0.4–3.9)
Average ^{18}F-fluoroestradiol SUV$_{max}$	3.2 (0.9–10.1)

*Geometric mean of up to 3 lesions with highest ^{18}F-FDG SUV$_{max}$.
Qualitative data are numbers followed by percentages in parentheses; continuous data are median followed by range in parentheses.

Patient-level ^{18}F-FDG uptake summary =

$$\text{antilog}\left[\left(\sum_{1}^{n_i} \log(^{18}\text{F} - \text{FDG } \text{SUV}_{max})/n_i\right)\right] \text{ Eq. 2}$$

The percentage change in uptake from baseline between ^{18}F-fluoroestradiol and ^{18}F-FDG PET scans was computed at the lesion level and for patient-level summaries.

Statistical Methods

The primary objective was to estimate the extent of clinical benefit, defined as freedom from progressive disease for 6 mo after the start of therapy. In the original protocol (sequential cohort), a clinical benefit in 3 or more of 20 patients would indicate a promising treatment. The amended protocol (simultaneous cohort) updated the criteria to clinical benefit in 2 or more of 14 patients (so that the lower bound of a 90% score CI would exceed the null rate of 5%). Secondary objectives included assessment of safety, PFS, and overall survival (OS) from the start of study therapy; restoration of endocrine sensitivity (by ^{18}F-fluoroestradiol PET); and tumor metabolic response (by ^{18}F-FDG PET). Restoration of endocrine sensitivity (i.e., an increase in ER expression measured by radioligand binding) could be indicated by qualitative ^{18}F-fluoroestradiol

uptake above background levels at a postbaseline scan for a lesion that was qualitatively ^{18}F-fluoroestradiol–negative at baseline, or by passing an arbitrary threshold of a 20% increase in ^{18}F-fluoroestradiol SUL$_{mean}$. Lesion-level analysis of time trends in ^{18}F-fluoroestradiol and ^{18}F-FDG uptake (log-transformed) and relationships with clinical benefit used linear mixed-effects models with patient- and lesion-level random intercepts.

RESULTS

Eight patients enrolled in the sequential cohort; 16 patients enrolled in the simultaneous cohort, including 1 patient later identified as a screening failure who never received study therapy. Table 1 describes the characteristics of the treated patients in each cohort. All patients were female; most had extensive prior exposure to both endocrine therapy (range, 2–6 lines) and cytotoxic chemotherapy (range, 1–10 lines). The number of lesions ranged from 1 to 10 for all patients in both cohorts, and the location of metastases was not a reason for exclusion. Individual patient imaging and efficacy data are shown in Supplemental Tables 2 and 3.
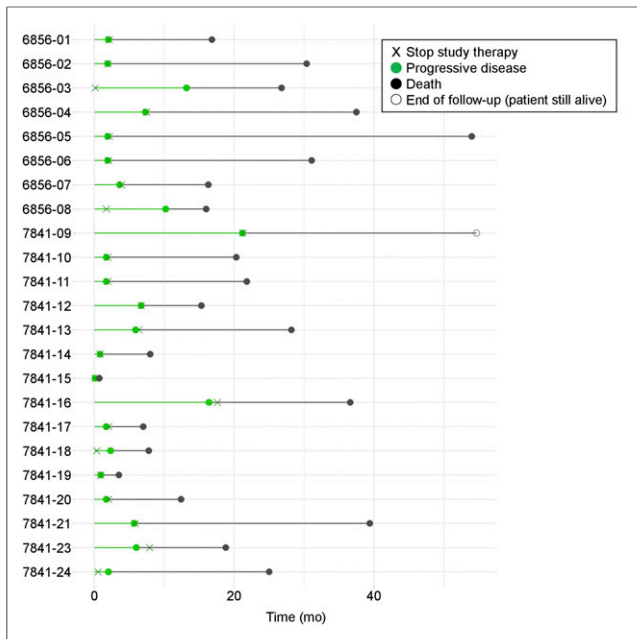
FIGURE 2. PFS and OS per patient (6,856 = sequential cohort; 7,841 = simultaneous cohort).

Efficacy Analysis

In the sequential cohort ($n = 8$), 2 patients withdrew during cycle 1 because of vorinostat toxicity (grade 3 fatigue) and were not evaluable for week 8 response. Four patients had progressive disease at week 8, and 2 patients had stable disease at week 8 (33%; 90% CI, 12%–65%), with eventual progression at 4 and 7 mo from the start of therapy.

In the simultaneous cohort ($n = 15$), 5 patients were not evaluable for week 8 response: 2 had rapidly progressing disease during cycle 1, and 3 chose to withdraw from study treatment because of adverse events, including grade 3 hyperglycemia, grade 3 dizziness, and grade 2 rigor or chills. Four of the remaining 10 patients had progressive disease at week 8; the proportion of evaluable

patients with stable disease at week 8 was therefore 60% (90% CI, 35%–81%). Four patients in the simultaneous cohort experienced clinical benefit for at least 6 mo on study therapy without progressive disease.

PFS and OS are reported for each patient in Figure 2. The median PFS for the 8 patients in the sequential cohort was 3 mo (range, 2–13 mo), and the median OS was 29 mo (range, 16–54 mo). In the simultaneous cohort, the median PFS was 2 mo (range, 0–21 mo); OS includes 1 patient still alive 55 mo after starting study therapy; a Kaplan–Meier estimate of median OS is 19 mo (range, 1–55 mo).

Toxicity

Twenty-five adverse events were recorded in 12 of the 23 patients. Grade 3 and 4 adverse events are listed in Table 2, with the full list presented in Supplemental Table 4. Most adverse events, including grade 3 fatigue and grade 2 nausea or vomiting likely related to vorinostat, occurred during the first month and were self-limiting with supportive care. Side effects at later cycles were uncommon; renal insufficiency led to a vorinostat dose reduction at 161 d, and another patient had muscle cramps also at 161 d (for which vorinostat was withheld and then reduced), followed by an unrelated fracture at 496 d. No adverse events occurred as a result of ^{18}F-fluoroestradiol imaging.

Imaging

Both ^{18}F-fluoroestradiol and ^{18}F-FDG PET imaging were completed before therapy, after week 2, and after week 8, unless patients had already gone off study therapy (2 patients in the sequential cohort and 5 in the simultaneous cohort), or when ^{18}F-fluoroestradiol PET (2 sequential, 4 simultaneous) or ^{18}F-FDG PET (1 simultaneous) was not performed because of scheduling or other difficulties. Patient-level geometric means for ^{18}F-fluoroestradiol SUL$_{mean}$ and ^{18}F-FDG SUV$_{max}$ for up to 3 lesions with the highest baseline ^{18}F-FDG SUV$_{max}$ are shown in Figure 3. Lesion-level data are displayed in Supplemental Figure 1. The median value of the geometric means for baseline ^{18}F-FDG SUV$_{max}$ for the 3 most ^{18}F-FDG–avid lesions was 4.9 (range, 2.7–12.8). All these baseline ^{18}F-FDG uptake summaries were above our previously determined

TABLE 2
Grade 3+ Toxicity Summary

Patient no.	Toxicity	Grade	SAE?	Days on vorinostat	Relation to vorinostat	Relation to AI
Sequential cohort						
3	Fatigue	3	No	3	Very likely	Not related
6	Flulike syndrome	3	Yes	24	Not related	Not related
8	Fatigue	3	No	10	Very likely	Not related
Simultaneous cohort						
14	Dizziness	3	No	4	Possible	Doubtful
15	Liver dysfunction/failure	4	Yes	4	Not related	Not related
23	Hypermagnesemia	3	No	19	Doubtful	Not related
23	Neutrophils	3	No	19	Very likely	Not related
24	Diarrhea	3	No	1	Very likely	Not related
24	Hyperglycemia	3	No	7	Possible	Not related

SAE = serious adverse event.
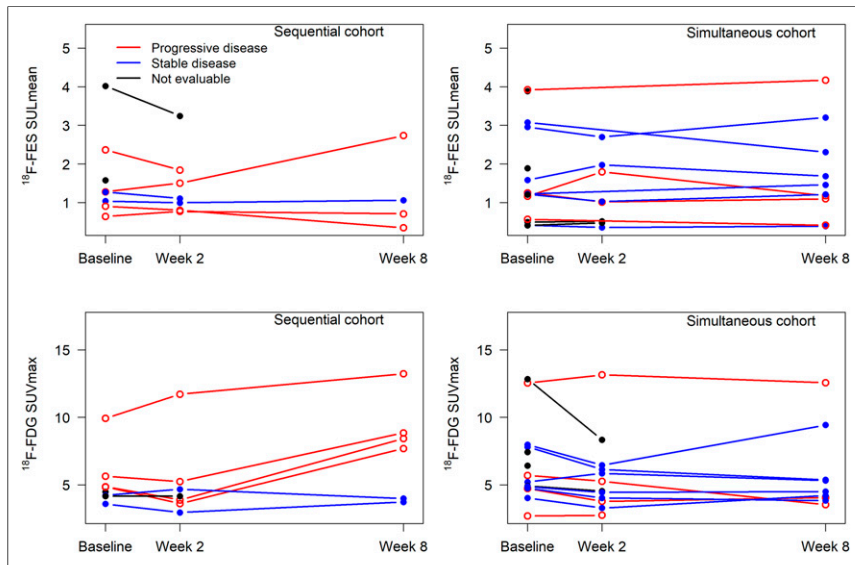
FIGURE 3. Geometric mean ^{18}F-fluoroestradiol SUL_{mean} and ^{18}F-FDG SUV_{max} for up to 3 lesions per patient (highest baseline ^{18}F-FDG SUV_{max}) in sequential and simultaneous cohorts.

threshold of 2.2 (*23*), suggesting glycolytically active, relatively aggressive disease. The median value for ^{18}F-fluoroestradiol SUL_{mean} geometric mean (the 3 most ^{18}F-FDG–avid lesions) was 1.3 (range, 0.4–4.0). Most patients (18/23, 78%) had a baseline average ^{18}F-fluoroestradiol SUL_{mean} of at least 0.85 (*23*). Patients with a baseline average ^{18}F-fluoroestradiol ($SUL_{mean} \geq 0.85$) had a higher average PFS (median, 2.9 mo; 95% CI, 1.9–6.7) than patients with a baseline ^{18}F-fluoroestradiol SUL_{mean} of less than 0.85 (median, 1.7 mo; 95% CI, 0.8–5.9) (log-rank $P = 0.036$) (Supplemental Fig. 2). In qualitative assessments, baseline ^{18}F-fluoroestradiol uptake was at or below the background level for all lesions in 4 of the 5 scans with a geometric mean ^{18}F-fluoroestradiol SUL_{mean} of less than 0.85 (Supplemental Table 2). In the fifth scan, 1 lung lesion (quantitative SUL_{mean}, 0.94) was above the background level and 1 (quantitative SUL_{mean}, 0.43) was not. Single qualitatively ^{18}F-fluoroestradiol–negative lesions in patients with 3 or more ^{18}F-fluoroestradiol–positive lesions occurred in 2 other cases (Supplemental Table 2).

Vorinostat did not systematically increase ^{18}F-fluoroestradiol uptake for patients in either cohort. For example, of 5 patients with fluoroestradiol-negative (geometric mean ^{18}F-fluoroestradiol SUL, <0.85) imaging at baseline, none had an average ^{18}F-fluoroestradiol SUL_{mean} of 0.85 or more on any subsequent scan (Supplemental Table 2). Three patients had a more than 20% increase in geometric mean ^{18}F-fluoroestradiol SUL from baseline to 2 wk, but none maintained this increase at 8 wk. One patient who did not have an increase at the 2-wk scan had a more than 20% increase in geometric mean ^{18}F-fluoroestradiol SUL at 8 wk. Representative ^{18}F-fluoroestradiol and ^{18}F-FDG image examples are shown for a patient with progressive disease (Fig. 4) and with clinical response (Fig. 5).

Associations between imaging measures and the primary endpoint (clinical benefit, PFS ≥ 6 mo) were explored further in the simultaneous cohort (the primary efficacy analysis cohort). Analysis of 86 lesions in 15 patients corroborated observations from the patient-level descriptive analysis. Baseline or pretreatment ^{18}F-fluoroestradiol SUL_{mean} was estimated to be 171% higher ($P = 0.03$; 95% CI, 11%–565%) for patients with clinical benefit (baseline fitted average,

2.7; 95% CI,1.2–6.0) than without (baseline fitted average, 1.0; 95% CI, 0.7–1.5). Average baseline ^{18}F-FDG SUV_{max} did not differ between patients with and without 6-mo clinical benefit (Wald test, $P = 0.84$). Clinical benefit was also not associated with a decrease in ^{18}F-FDG SUV_{max} (Supplemental Fig. 1).

DISCUSSION

In this study, ^{18}F-fluoroestradiol and ^{18}F-FDG measures were stable over 8 wk of therapy; ^{18}F-fluoroestradiol or ^{18}F-FDG uptake changes were not a marker of clinical benefit. This finding may be expected, since stable disease rather than tumor regression (*26*) was the criterion for treatment benefit, and many of the lesions were in bone, where progression is often slower than in visceral metastases (*29*).

The combination of an HDACI (vorinostat) and an AI is an active and durable treatment regimen for ER+/human epidermal growth factor receptor 2 (HER2)–negative metastatic breast cancer. Despite prior disease progression on prior endocrine therapy, approximately half of evaluable patients had stable disease at 8 wk, with 40% of patients in the simultaneous cohort remaining on treatment for more than 6 mo. Two patients had an extended benefit of 16 and 21 mo until progression. These results are consistent with other phase II studies combining HDACIs and endocrine therapy (*17*). The combination of vorinostat and AI was relatively well tolerated, and AIs were recycled; thus, the observed benefit is likely from the activity of vorinostat or synergy with the AI.

There are limitations to this study. Although several lesions were available per patient for evaluation, the total number of patients
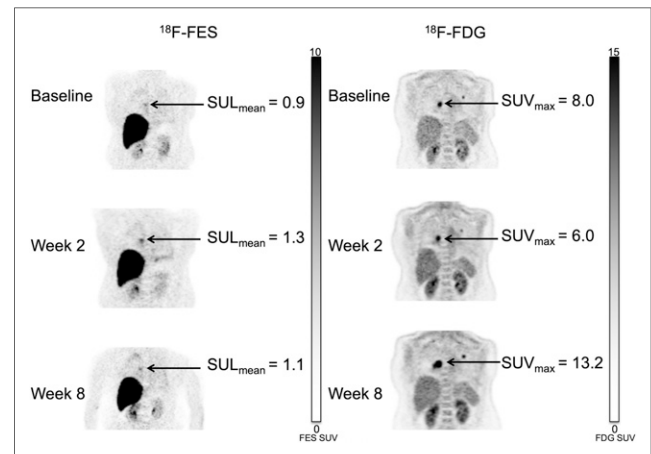
FIGURE 4. 47-y-old woman in sequential cohort (patient 2). Patient had 2 metastases from invasive ductal carcinoma to lung. Primary lesion was ER-positive, PR-positive, and HER2-negative. Although ^{18}F-fluoroestradiol SUL_{mean} rose slightly and ^{18}F-FDG SUV_{max} decreased after 2 wk of therapy, lesion size appeared stable. At 8 wk, with more than doubling of ^{18}F-FDG SUV_{max} from second scan, RECIST measure showed 37% increase in lesion size, indicating progressive disease.
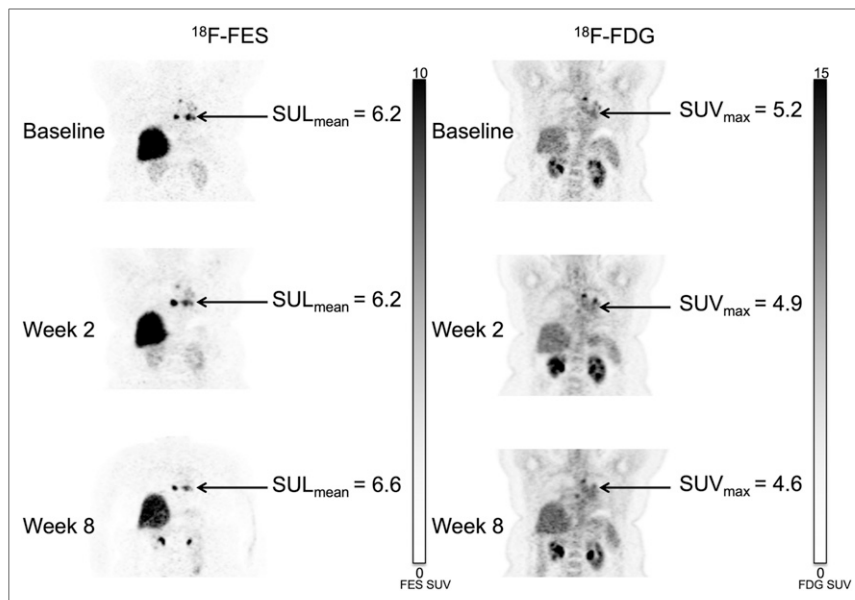
FIGURE 5. Mediastinal lymph node lesions in 53-y-old woman in simultaneous cohort (patient 12). Patient had history of ER-positive, PR-positive, HER2-negative invasive ductal carcinoma in right breast. Uptake on both ^{18}F-fluoroestradiol and ^{18}F-FDG imaging remained stable through all 3 time points. RECIST measures also showed stable disease. She remained on study therapy for 6.7 mo until disease progression.

evaluated was small ($n = 23$), and not all patients completed the study (some because of vorinostat toxicity). In addition, contemporaneous tissue biopsy of each lesion cannot be available as a biomarker to predict efficacy. Restoration of endocrine sensitivity was defined both qualitatively and quantitatively, but it is necessary to note that ^{18}F-fluoroestradiol measures the functional ability of ER to bind and concentrate ligand, and ER is not, by itself, a marker of sensitivity. It is also important to note that rigorous protocols are needed to ensure measurement precision. Our centers implement a qualification process using National Institute of Standards and Technology–traceable reference sources for scanners and dose calibrators, regular calibration, and common patient and imaging protocols yielding highly reproducible SUV measurements (*34,35*).

Study inclusion criteria selected patients who had benefitted from endocrine therapy before developing resistance. It is expected that we would see ER expression, but the question remains as to whether this predicts response to endocrine (recycled) therapy plus a molecularly targeted agent such as vorinostat. We suspect that persistent ER binding measured by ^{18}F-fluoroestradiol shows a likelihood of endocrine clinical benefit. A challenge in managing these patients is that multiple pathways may override the endocrine sensitivity, which would explain persistent ER function measured by ^{18}F-fluoroestradiol in the face of progressive disease.

This study validates prior observations that baseline high ^{18}F-fluoroestradiol predicts PFS on later-line AI therapy (here in combination with vorinostat), with the qualitative status of "most lesions" as an accurate patient-level summary of ^{18}F-fluoroestradiol uptake (*36*).

Serial ^{18}F-fluoroestradiol and ^{18}F-FDG PET imaging can be used to monitor the effect of the combination of an HDACI (vorinostat) and an AI on ER expression and tumor glycolytic rate in metastatic breast cancer.

CONCLUSION

We found that ^{18}F-fluoroestradiol PET predicts response to HDACI/AI therapy and that ^{18}F-fluoroestradiol uptake remains stable during the initial 8 wk of treatment. This study also suggests that the addition of vorinostat to AI in patients with ER+ breast cancer results in tumor response or stable disease in about half of evaluable patients who had progressed on prior endocrine therapies. Our results support further study of serial molecular imaging along with combined HDACIs and AI therapy (such as ECOG-ACRIN study E2112), to further delineate the role of HDACIs and potential biomarkers in AI-refractory ER+ advanced breast cancer.

KEY POINTS

QUESTION: Can molecular imaging (^{18}F-fluoroestradiol and ^{18}F-FDG PET) be used to image the potential resensitization of ERs in ER+ metastatic breast cancer patients who received therapy with an HDACI and an AI?

PERTINENT FINDINGS: Higher ^{18}F-fluoroestradiol PET uptake at baseline predicted response to HDACIs/AI therapy. The addition of vorinostat to AI in patients with ER+ breast cancer resulted in tumor response or stable disease in about half of evaluable patients who had progressed on prior endocrine therapies.

IMPLICATIONS FOR PATIENT CARE: Serial molecular imaging along with combined HDACI and AI therapy may further delineate the role of HDACIs and potential biomarkers in AI-refractory ER+ advanced breast cancer.

REFERENCES

1. Carlson RW, Anderson BO, Burstein HJ, et al. Invasive breast cancer. *J Natl Compr Canc Netw.* 2007;5:246–312.

2. Hanamura T, Hayashi SI. Overcoming aromatase inhibitor resistance in breast cancer: possible mechanisms and clinical applications. *Breast Cancer.* 2018;25:379–391.

3. NCCN guideline update: breast cancer version 1.2004. *J Natl Compr Canc Netw.* 2004;2:183–184.

4. Turner NC, Ro J, Andre F, et al. Palbociclib in hormone-receptor-positive advanced breast cancer. *N Engl J Med.* 2015;373:209–219.

5. Piccart M, Hortobagyi GN, Campone M, et al. Everolimus plus exemestane for hormone-receptor-positive, human epidermal growth factor receptor-2-negative advanced breast cancer: overall survival results from BOLERO-2. *Ann Oncol.* 2014;25:2357–2362.

6. André F, Ciruelos E, Rubovszky G, et al. Alpelisib for PIK3CA-mutated, hormone receptor-positive advanced breast cancer. *N Engl J Med.* 2019;380:1929–1940.

7. Raha P, Thomas S, Thurn KT, Park J, Munster PN. Combined histone deacetylase inhibition and tamoxifen induces apoptosis in tamoxifen-resistant breast cancer models, by reversing Bcl-2 overexpression. *Breast Cancer Res.* 2015;17:26.

8. Fan J, Yin WJ, Lu JS, et al. ER alpha negative breast cancer cells restore response to endocrine therapy by combination treatment with both HDAC inhibitor and DNMT inhibitor. *J Cancer Res Clin Oncol.* 2008;134:883–890.

9. Giacinti L, Claudio PP, Lopez M, Giordano A. Epigenetic information and estrogen receptor alpha expression in breast cancer. *Oncologist.* 2006;11:1–8.

10. Jang ER, Lim SJ, Lee ES, et al. The histone deacetylase inhibitor trichostatin A sensitizes estrogen receptor alpha-negative breast cancer cells to tamoxifen. *Oncogene.* 2004;23:1724–1736.

11. Lee YJ, Won AJ, Lee J, et al. Molecular mechanism of SAHA on regulation of autophagic cell death in tamoxifen-resistant MCF-7 breast cancer cells. *Int J Med Sci.* 2012;9:881–893.

12. Thomas S, Thurn KT, Bicaku E, Marchion DC, Munster PN. Addition of a histone deacetylase inhibitor redirects tamoxifen-treated breast cancer cells into apoptosis, which is opposed by the induction of autophagy. *Breast Cancer Res Treat.* 2011;130:437–447.

13. Connolly R, Stearns V. Epigenetics as a therapeutic target in breast cancer. *J Mammary Gland Biol Neoplasia.* 2012;17:191–204.

14. Krusche CA, Wulfing P, Kersting C, et al. Histone deacetylase-1 and -3 protein expression in human breast cancer: a tissue microarray analysis. *Breast Cancer Res Treat.* 2005;90:15–23.

15. Sabnis GJ, Goloubeva O, Chumsri S, Nguyen N, Sukumar S, Brodie AM. Functional activation of the estrogen receptor-alpha and aromatase by the HDAC inhibitor entinostat sensitizes ER-negative tumors to letrozole. *Cancer Res.* 2011;71:1893–1903.

16. Yardley DA, Ismail-Khan RR, Melichar B, et al. Randomized phase II, double-blind, placebo-controlled study of exemestane with or without entinostat in postmenopausal women with locally recurrent or metastatic estrogen receptor-positive breast cancer progressing on treatment with a nonsteroidal aromatase inhibitor. *J Clin Oncol.* 2013;31:2128–2135.

17. Munster PN, Thurn KT, Thomas S, et al. A phase II study of the histone deacetylase inhibitor vorinostat combined with tamoxifen for the treatment of patients with hormone therapy-resistant breast cancer. *Br J Cancer.* 2011;104:1828–1835.

18. Yeruva SLH, Zhao F, Miller KD, et al. E2112: randomized phase iii trial of endocrine therapy plus entinostat/placebo in patients with hormone receptor-positive advanced breast cancer. *NPJ Breast Cancer.* 2018;4:1.

19. Peterson LM, Mankoff DA, Lawton T, et al. Quantitative imaging of estrogen receptor expression in breast cancer with PET and ^{18}F-fluoroestradiol. *J Nucl Med.* 2008;49:367–374.

20. Koleva-Kolarova RG, Greuter MJ, van Kruchten M, et al. The value of PET/CT with FES or FDG tracers in metastatic breast cancer: a computer simulation study in ER-positive patients. *Br J Cancer.* 2015;112:1617–1625.

21. Gong C, Yang Z, Sun Y, et al. A preliminary study of ^{18}F-FES PET/CT in predicting metastatic breast cancer in patients receiving docetaxel or fulvestrant with docetaxel. *Sci Rep.* 2017;7:6584.

22. He S, Wang M, Yang Z, et al. Comparison of ^{18}F-FES, ^{18}F-FDG, and ^{18}F-FMISO PET imaging probes for early prediction and monitoring of response to endocrine therapy in a mouse xenograft model of ER-positive breast cancer. *PLoS One.* 2016;11:e0159916.

23. Kurland BF, Peterson LM, Lee JH, et al. Estrogen receptor binding (^{18}F-FES PET) and glycolytic activity (^{18}F-FDG PET) predict progression-free survival on endocrine therapy in patients with ER+ breast cancer. *Clin Cancer Res.* 2017;23:407–415.

24. Linden HM, Kurland BF, Peterson LM, et al. Fluoroestradiol positron emission tomography reveals differences in pharmacodynamics of aromatase inhibitors, tamoxifen, and fulvestrant in patients with metastatic breast cancer. *Clin Cancer Res.* 2011;17:4799–4805.

25. Connolly RM, Leal JP, Goetz MP, et al. TBCRC 008: early change in ^{18}F-FDG uptake on PET predicts response to preoperative systemic therapy in human epidermal growth factor receptor 2-negative primary operable breast cancer. *J Nucl Med.* 2015;56:31–37.

26. Kurland BF, Gadi VK, Specht JM, et al. Feasibility study of FDG PET as an indicator of early response to aromatase inhibitors and trastuzumab in a heterogeneous group of breast cancer patients. *EJNMMI Res.* 2012;2:34.

27. Ulaner GA, Eaton A, Morris PG, et al. Prognostic value of quantitative fluorodeoxyglucose measurements in newly diagnosed metastatic breast cancer. *Cancer Med.* 2013;2:725–733.

28. Zhang J, Jia Z, Zhang Y, et al. The maximum standardized uptake value of ^{18}F-FDG PET scan to determine prognosis of hormone-receptor positive metastatic breast cancer. *BMC Cancer.* 2013;13:42.

29. Peterson LM, O'Sullivan J, Wu QV, et al. Prospective study of serial ^{18}F-FDG PET and ^{18}F-fluoride PET to predict time to skeletal-related events, time to progression, and survival in patients with bone-dominant metastatic breast cancer. *J Nucl Med.* 2018;59:1823–1830.

30. Kelly WK, O'Connor OA, Krug LM, et al. Phase I study of an oral histone deacetylase inhibitor, suberoylanilide hydroxamic acid, in patients with advanced cancer. *J Clin Oncol.* 2005;23:3923–3931.

31. Luu TH, Morgan RJ, Leong L, et al. A phase II trial of vorinostat (suberoylanilide hydroxamic acid) in metastatic breast cancer: a California Cancer Consortium study. *Clin Cancer Res.* 2008;14:7138–7142.

32. Linden HM, Stekhova SA, Link JM, et al. Quantitative fluoroestradiol positron emission tomography imaging predicts response to endocrine treatment in breast cancer. *J Clin Oncol.* 2006;24:2793–2799.

33. *Research on Obesity: A Report of the DHSS/MRC Group.* Her Majesty's Stationary Office; 1976:94.

34. Byrd DW, Doot RK, Allberg KC, et al. Evaluation of cross-calibrated [68]Ge/^{68}Ga phantoms for assessing PET/CT measurement bias in oncology imaging for single- and multicenter trials. *Tomography.* 2016;2:353–360.

35. Kurland BF, Peterson LM, Shields AT, et al. Test-retest reproducibility of ^{18}F-FDG PET/CT uptake in cancer patients within a qualified and calibrated local network. *J Nucl Med.* 2019;60:608–614.

36. Venema CM, Apollonio G, Hospers GA, et al. Recommendations and technical aspects of 16α-[^{18}F]fluoro-17β-estradiol PET to image the estrogen receptor in vivo: the Groningen experience. *Clin Nucl Med.* 2016;41:844–851.